JACS
JOURNAL OF THE AMERICAN CHEMICAL SOCIETY
Article
pubs.acs.org/JACS

DNA-Mediated Assembly of Protein Heterodimers on Membrane Surfaces

Michael P. Coyle,[†,‡,§] Qian Xu,[†,‡,§,⊥] Samantha Chiang,[†] Matthew B. Francis,*[,†,§] and Jay T. Groves*[,†,‡,§]

[†]Department of Chemistry and [‡]Howard Hughes Medical Institute, University of California, Berkeley, California 94720, United States
[§]Physical Biosciences and Materials Sciences Divisions, Lawrence Berkeley National Laboratory, Berkeley, California 94720, United States

Supporting Information

ABSTRACT: We present a method based on self-assembling oligonucleotides to anchor proteins to a supported membrane surface. This anchoring method allows control of the surface density of multiple proteins. By incorporating additional recognition sequences into the DNA linkers, defined heterodimers can be produced upon the addition of a heterospecific DNA cross-linking strand. Characterization by fluorescence cross-correlation spectroscopy (FCCS) confirmed lateral mobility and the formation of specific heterodimers. We further demonstrate that proteins linked in this manner as either monomers or dimers can form functional interfaces with living cells.

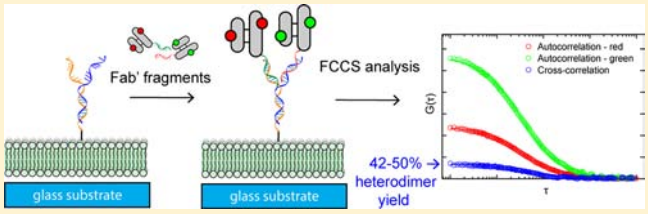

INTRODUCTION

Numerous biological processes, including immune recognition,[1−3] animal development,[4−8] and the misregulation of development in cancer cell progression,[9] involve signaling interactions across cell−cell junctions. In this juxtacrine configuration, ligands and receptors bind to each other from apposed cell surfaces. Supported lipid membranes can reconstitute functional juxtacrine signaling interfaces with living cells and have been a useful tool to study and manipulate these interactions.[10−19] Protein ligands that would naturally occur on one cell surface are instead synthetically coupled to the supported membrane. The lateral mobility of the supported membrane enables these ligands to diffuse and assemble into functional clusters as they engage their cognate ligands on the adjacent live cell surface. Such signaling clusters are emerging as a general phenomenon common to many juxtacrine signaling interactions.[20−22] Recent studies on the Eph[23−26] and EGFR[27−29] families of receptor tyrosine kinases (RTKs) indicate that heterooligomerization of proteins within signaling clusters may exert additional layers of regulatory control. The increasing numbers of therapeutic bispecific antibodies entering clinical trials[30,31] suggest that it may be possible to modulate signaling cluster content with therapeutic benefit. With the goal of extending the utility of supported membranes for the study of complex, multicomponent clusters and the demonstrated success of DNA-based protein assembly,[32−38] we report here a DNA-based assembly strategy to associate proteins with membranes and to control their assembly into defined heterodimers or higher-order oligomers.

RESULTS AND DISCUSSION

Thiol-functionalized DNA was coupled to maleimide-functionalized supported membranes. Unlike strategies that incorporate long alkyl chains onto DNA during solid-phase synthesis,[39,40] this strategy permitted DNA conjugation to preformed membranes. In this study, supported membranes with a 1:20 molar ratio of maleimide functionalized phospholipids to 1,2-dioleoyl-*sn*-glycero-3-phosphocholine were used. The supported membrane was prepared in phosphate buffered saline (PBS, 10 mM phosphate buffer, 150 mM NaCl) by vesicle deposition on clean glass, as described in the Supporting Information (SI). Attachment of the DNA and lateral fluidity of the membrane were confirmed by fluorescence recovery after photobleaching (FRAP) after treating the supported membrane with 20 nt single-stranded DNA (ssDNA) bearing a 5′-thiol modifier and a 3′-6-carboxyfluorescein (FAM) moiety (Figure 1a).

The surface density of conjugated DNA was quantified using membrane standards with known lipid fluorophore surface densities (Figure S1 in the SI).[41] Conjugation of 20 nt and 41 nt ssDNA to supported membranes and hybridization of TEX615 or Alexa Fluor 488 (AF488) labeled complementary strands to the resulting samples allowed quantification of the DNA on the membrane surface by comparing the observed fluorescence intensities of the DNA samples to those of the membrane standards. Surface density of DNA increased proportionally to the concentration of thiol DNA that was applied (Figure 1b). With incubation concentrations of DNA in the low micromolar range, surface densities in the range 0−3000 strands/μm^2 were observed. The density of many cell surface proteins is <3000 molecules/μm^2.[13,42−45] Addition of thiol DNA in concentrations above 6 μM resulted in further increases in measured surface density; however, larger

Received: October 12, 2012
Published: March 26, 2013

   dx.doi.org/10.1021/ja3101215 | *J. Am. Chem. Soc.* 2013, 135, 5012−5016

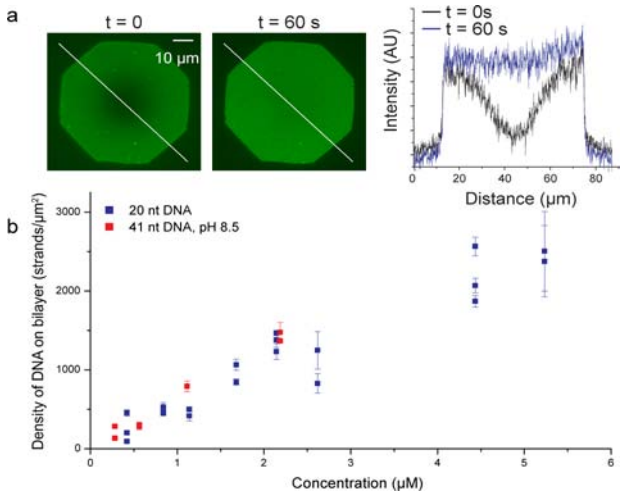

Figure 1. Conjugation of DNA oligonucleotides to a supported membrane. (a) A representative FRAP characterization of a supported membrane with fluorescently labeled ssDNA is shown. The scale bar represents 10 μm. The graph shows the intensity profiles along the white lines. (b) The surface density of coupled DNA can be varied over a large concentration range. The error bars represent the standard error of the mean from multiple images.

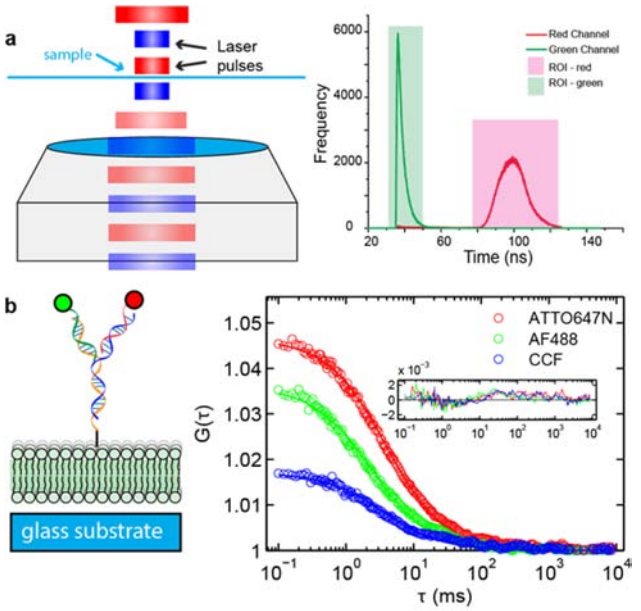

c

Sample	$G(0)_x/\min(G(0)_r, G(0)_g)$
Heterodimer	0.46 - 0.48
Negative control	0.00 - 0.03
Dual labeled ssDNA	0.80 - 0.88

Figure 2. Analysis of fluorophore heterodimers with FCCS. (a) A diagram is shown for a PIE-FCCS experiment. Excitation light is interleaved to allow time-resolved data collection, as shown in the graph, and thus removal of the contribution of fluorescence signal bleedthrough to cross-correlation. (b) FCCS analysis indicated the codiffusion of the DNA-bound fluorophores, suggesting that they had formed a heterodimer. Fits to the data are shown as solid lines. Fit residuals are shown in the inset in the corresponding colors. (c) The table compares the relative cross-correlation amplitudes to the lower of the two autocorrelation amplitudes, including positive and negative control samples (shown in SI, Figure S5).

variations between identical samples were observed, and the relationship between surface density and incubation concentration became nonlinear. ssDNA, 41 nt, coupled to the supported membrane less efficiently than 20 nt ssDNA under the same conditions (PBS, pH 7.4), but the use of pH 8.5 borate buffered saline (BBS, 10 mM borate, 150 mM NaCl) as a higher pH buffer yielded surface densities of 41 nt ssDNA very similar to those of 20 nt ssDNA coupled at the lower pH (Figure 1b).

For the assembly of more complex structures, we designed DNA heterodimers using previously published assembly sequences.[46−48] Several strand configurations were evaluated, as shown in SI, Figure S3. Of these, a particularly successful strategy for the formation of four-strand "Y"-shaped structures was selected (Figure 2b and SI, Figure S4).

The two arms of the branched structures were labeled with green and red fluorophores, as shown in Figure 2b, allowing characterization by two-color fluorescence cross-correlation spectroscopy (FCCS)[49] with pulsed interleaved excitation (PIE,[50] see Figure 2a and experimental diagram in SI, Figure S2). FCCS has been used to characterize binding characteristics of biomolecules,[51,52] enzymatic activity,[53] and clustering in cell membranes.[54] PIE eliminates artifactual cross-correlation from fluorescence spectral bleed-through by exciting the sample with interleaved laser pulses. The red peak is broad since pulsing is achieved through electro-optic modulation of a continuous wave KrAr laser. The amplitude of the cross-correlation function is proportional to the concentration of dual-labeled species. Measurement of this parameter can be obscured by a variety of artifacts that can both raise or lower the measured cross-correlation amplitude.[55] Using control samples that establish the upper and lower bounds of the cross-correlation measurement enables calibration of the cross-correlation signal and quantification of the amount of heterodimer formed (SI and Figure S5).[52] Performing this analysis of the data shown in Figure 2c provides an estimate of 52−60% yield of assembled heterodimer.

Formation of protein heterodimers was demonstrated by assembling heterodimers of Fab′ fragment−DNA conjugates, effectively reconstructing membrane-bound antibodies. Fab′ fragments can be generated from IgG antibodies, which are readily obtained against many proteins. For this study, $F(ab')_2$ fragments generated from polyclonal donkey anti-mouse antibodies were obtained from a commercial source, labeled with fluorophores, and partially reduced with 2-mercaptoethylamine (2-MEA) to produce Fab′ fragments with free thiol groups at the C-terminal regions, Figure 3a.[56,57] The products were thoroughly desalted and treated with maleimide-functionalized 20 nt ssDNA (see SI for procedures and Figure S6 for MALDI-TOF MS characterization data). The conjugates were purified by size exclusion chromatography (Figure 3b) and analyzed by gel electrophoresis (SDS-PAGE, Figure 3c). Separation of the proteins from free ssDNA is shown in the chromatogram (Figure 3b). After treating the Fab′ fragments with maleimide DNA, gel electrophoresis analysis indicated a species with higher molecular weight compared to the unmodified Fab′ fragments (Figure 3c). These conjugates were prepared with different sequences of DNA and labeled with distinct fluorophores so that a heterodimer could be prepared on DNA-functionalized supported membranes, as shown in Figure 3d. The resulting structure was then analyzed by FCCS to measure heterodimerization (Figure 3e). By

dx.doi.org/10.1021/ja3101215 | J. Am. Chem. Soc. 2013, 135, 5012−5016

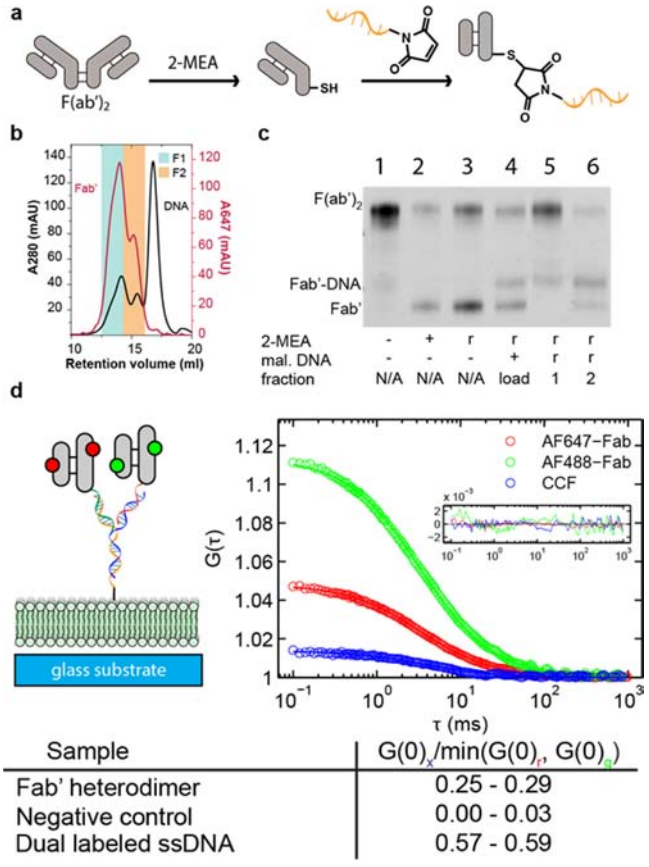

Sample	$G(0)_x/\min(G(0)_r, G(0)_g)$
Fab' heterodimer	0.25 - 0.29
Negative control	0.00 - 0.03
Dual labeled ssDNA	0.57 - 0.59

Figure 3. Fab′−DNA conjugates can be cross-linked on SLBs. (a) A scheme is shown for Fab′−DNA conjugate synthesis. (b) SEC separations were performed for AF647-labeled Fab−DNA conjugates. (c) An SDS-PAGE gel of (1) $F(ab')_2$. (2) Fab′ before removal of the 2-MEA reducing agent. (3) Fab′ after removal of the 2-MEA reducing agent. (4) Fab′ treated with maleimide DNA. (5) Highest molecular weight peak from SEC chromatography (blue shading), and (6) the intermediate molecular weight peak from SEC (orange shading). The entry "r" in the table indicates that the reagent has been removed, (d) FCCS analysis confirmed formation of a Fab′ heterodimer using the pooled fractions. Fits to the data are shown as solid lines. Fit residuals are shown in the inset.

comparing the cross correlation amplitude to that of a doubly labeled control sample, we determined that a 42−44% assembly yield was obtained for the heterodimeric structure. When expanded to antibody fragments with different specificities this technique provides a way to colocalize two different receptors using a convenient synthetic protocol.

Evaluation of nonspecific interactions between DNA functionalized membranes and living cells and accessibility of the DNA to presented cells was performed by modification of live Jurkat T-cells with surface ssDNAs, as described previously.[46] Cells were incubated with membranes functionalized with ssDNA sequences that were either complementary or noncomplementary to the cell surface ssDNA and a membrane of identical composition, but with no DNA functionalization. Upon washing, cells bound only to the membranes functionalized with complementary ssDNA. In addition, only one layer of cells was visible on the sample containing complementary DNA, while out-of-focus cells were visible in all samples before rinsing.

Presentation of a functional ligand for a cell surface receptor confirmed that membrane-anchored DNA is a useful anchor for protein presentation to live cells. EphinA1-YFP-His_{10}, which stimulates the EphA2 receptor when presented from supported membrane,[58] was linked to NTA_3−DNA.[59] This conjugate was subsequently hybridized to a supported membrane functionalized with complementary DNA. Fluorescence signal from the YFP portion of the protein−DNA conjugate confirmed the presence of the protein and FRAP analysis confirmed lateral mobility of the anchored protein. MDA-MB-231 cells were incubated with the EphrinA1-functionalized bilayers for 1 h, fixed with formaldehyde solution, and stained with an anti-EphA2 antibody. Analysis by total internal reflection fluorescence (TIRF) microscopy, which illuminates only the interface between the cell and the substrate, showed colocalization of the membrane-bound EphA2 receptors with EphrinA1, as expected from previous reports using biotin−streptavidin interactions or metal chelation.[13,58]

The ability to direct molecules into signaling clusters was demonstrated using epidermal growth factor (EGF) presented to MDA-MB-231 cells. While EGF is typically a soluble ligand, presentation to cells from a membrane surface results in visible clustering of the ligand.[60] Upon conjugation to Cy3-labeled DNA (Figure S8 in SI), hybridization of the conjugate to DNA functionalized membranes, and presentation to MDA-MB-231 cells, clustering of EGF and phosphorylation of EGFR were observed (Figure 4c). A Fab′ fragment that has no binding target on the cell membrane was not observed to undergo any change in localization caused by the cell. Presentation of a heterodimer of these molecules resulted in clustering of both, and no evidence of disruption of receptor phosphorylation was observed. These observations demonstrate that colocalization between anchored molecules can be directed independently of any inherent propensity of these molecules to colocalize.

We plan to use directed dimerization to study the effect of signaling cluster composition on EphA2 signaling. EphA2 has been observed to interact with other receptors in the Eph and EGFR families of RTKs.[26] To provide extra stability to the EphrinA1−DNA conjugate, we designed, expressed, and purified an EphrinA1−SNAPtag fusion and conjugated this molecule to DNA (Figure S9 in SI), a strategy also used in other studies.[32,61] EGF and EphrinA1 DNA conjugates were presented to MDA-MB-231 cells, which express both EGFR and EphA2 (Figure 5a). While the size of a DNA heterodimer is well below the diffraction limit, differences in colocalization between samples containing monomeric ligands and samples containing dimeric ligands could be observed (Figure 5b).

Analysis of fixed cells shows a clear difference in colocalization (Figure 5b, see SI and Figure S10 for a description of data analysis) between monomer and heterodimer presented samples. Since variations in the ligand distribution can be seen, we also expect to see differences in receptor distribution between cells presented with monomeric ligand and those presented with dimeric ligand. When staining the cells with an antibody against phosphorylated tyrosine 1173 (pY-EGFR) on the EGFR receptor, both colocalization measurements decrease, which is likely caused by incomplete antigen staining and some amount of nonspecific binding. Colocalization between the EphrinA1 ligand and the EGFR receptor is considerably increased in cells presented with a heterodimer, demonstrating that the EGFR is binding ligand and recruiting the EphrinA1 molecule. This observation suggests that the heterodimer is able to interact with the EGFR receptor and that ligand−receptor binding is preserved. A slight decrease in EGF−EGFR colocalization is observed in

dx.doi.org/10.1021/ja3101215 | J. Am. Chem. Soc. 2013, 135, 5012−5016

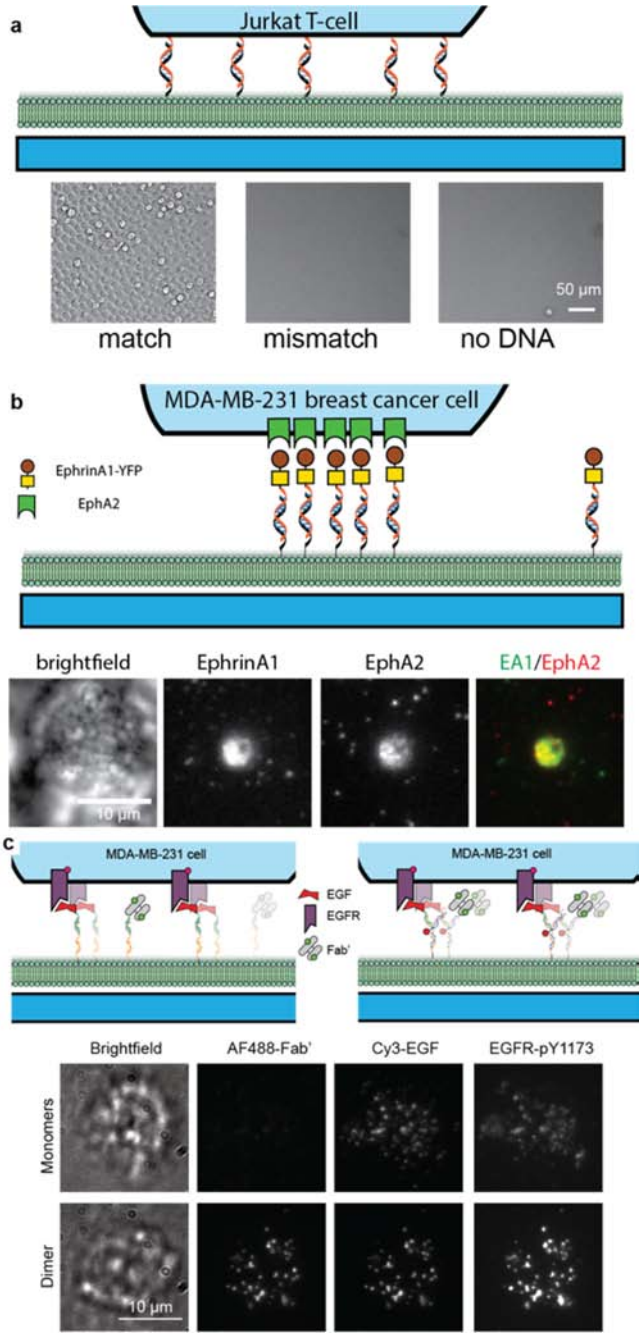

Figure 4. DNA-directed ligand display. (a) Nonadherent Jurkat T-cells functionalized with ssDNA attached only to membranes functionalized with complementary DNA strands. Few bound cells were observed on a maleimide-capped sample that lacked DNA. The scale bar represents 50 μm. (b) The DNA anchored EphrinA1-YFP-His_{10} construct stimulated MDA-MB-231 cells. In these images, EphA2 was stained with an antibody after cell permeabilization and imaged with TIRF microscopy. The scale bar represents 10 μm. (c) Heterodimeric protein complexes of EGF and an inert Fab′ fragment remain intact during interaction with MDA-MB-231 cells. Phosphorylation of the EGFR receptor is observed in both cases. The scale bar represents 10 μm.

the heterodimeric sample, relative to the monomeric control, suggesting that the interaction is somewhat inhibited. This possibility is under investigation. Additionally, we are are working to purify intact complexes from cell lysate by immunoprecipitation.

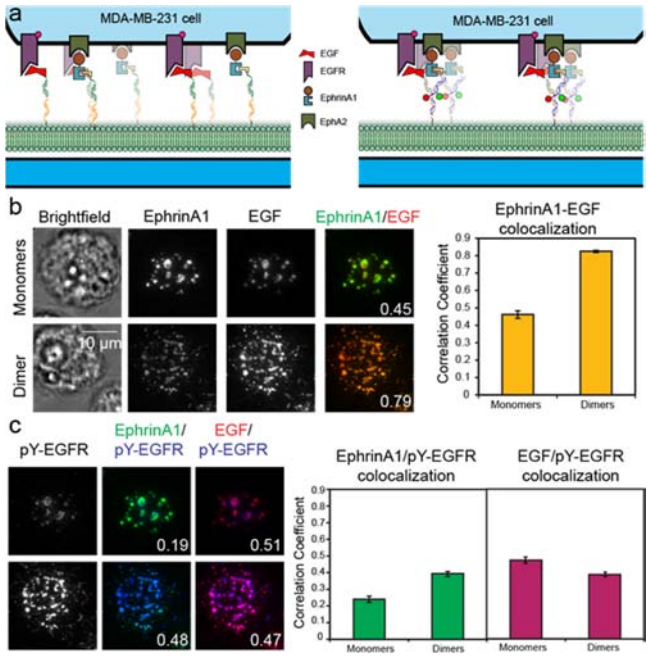

Figure 5. Alteration of receptor localization in cells. (a) MDA-MB-231 cells were deposited on supported membranes containing DNA bearing monomeric or dimeric ligand. (b) TIRF microscopy analysis demonstrates that the ligands appear segregated when presented as monomers but colocalized when presented as dimers. Colocalization was measured as the correlation coefficient in the EphrinAl clusters and is described in more detail in the SI. (c) Immunofluorescence staining of pTyr-1173 residue on EGFR of the cells in (b) shows that the receptor localization is altered by presentation of these ligands. The scale bar represents 10 μm, and the error bars depict the standard error of the mean. N(monomers) = 87, N(dimers) = 137. Numbers inset in the example images denote the actual correlation coefficient of the two channels shown in that particular image.

■ CONCLUSIONS

We have demonstrated the ability of DNA anchors extending from supported membranes to present functional protein ligands to cells and have also shown that this strategy is capable of generating heterodimeric structures that can direct the molecular composition of cell membrane receptor clusters.

■ ASSOCIATED CONTENT

Ⓢ Supporting Information

Full experimental procedures, image analysis workflow, and additional characterization data. This material is available free of charge via the Internet at http://pubs.acs.org.

■ AUTHOR INFORMATION

Corresponding Author

jtgroves@lbl.gov; mbfrancis@berkeley.edu

Present Address

[⊥]Department of Physics, University of Illinois at Urbana–Champaign, 1110 West Green Street, Urbana, IL 61801.

Notes

The authors declare no competing financial interest.

■ ACKNOWLEDGMENTS

We acknowledge Adam Smith, Christopher Rhodes, Il-Hyung Lee, and Sara Triffo for assistance with FCCS and data analysis. We also acknowledge Sonny Hsiao for assistance with Jurkat

cell culture and DNA-directed cell immobilization. This work was supported by the Director, Office of Science, Office of Basic Energy Sciences, Chemical Sciences, Geosciences and Biosciences Division of the U.S. Department of Energy under Contract No. DE-AC02_05CH11231. This research was partially funded by a National Institutes of Health NRSA Training Grant (1 T32 GMO66698) for M.P.C.

REFERENCES

(1) Watts, T. H.; Gaub, H. E.; McConnell, H. M. *Nature* **1986**, *320*, 179−181.
(2) Monks, C. R.; Freiberg, B. A.; Kupfer, H.; Sciaky, N.; Kupfer, A. *Nature* **1998**, *395*, 82−86.
(3) Dustin, M. L.; Groves, J. T. *Annu. Rev. Biophys.* **2012**, *41*, 543−556.
(4) Irvine, K. D.; Rauskolb, C. *Annu. Rev. Cell Dev. Biol.* **2001**, *17*, 189−214.
(5) Brachmann, R.; Lindquist, P. B.; Nagashima, M.; Kohr, W.; Lipari, T.; Napier, M.; Derynck, R. *Cell* **1989**, *56*, 691−700.
(6) Flanagan, J.; Vanderhaeghen, P. *Annu. Rev. Neurosci.* **1998**, *21*, 309−345.
(7) Wilkinson, D. G. *Nat. Rev. Neurosci.* **2001**, *2*, 155−164.
(8) Anklesaria, P.; Teixidó, J.; Laiho, M.; Pierce, J. H.; Greenberger, J. S.; Massagué, J. *Proc. Natl. Acad. Sci. U.S.A.* **1990**, *87*, 3289−3293.
(9) Pasquale, E. B. *Nat. Rev. Cancer* **2010**, *10*, 165−180.
(10) Grakoui, A.; Bromley, S. K.; Sumen, C.; Davis, M. M.; Shaw, A. S.; Allen, P. M.; Dustin, M. L. *Science* **1999**, *285*, 221−227.
(11) Mossman, K. D.; Campi, G.; Groves, J. T.; Dustin, M. L. *Science* **2005**, *310*, 1191−1193.
(12) Hartman, N. C.; Nye, J. A.; Groves, J. T. *Proc. Natl. Acad. Sci. U.S.A.* **2009**, *106*, 12729−12734.
(13) Salaita, K.; Nair, P. M.; Petit, R. S.; Neve, R. M.; Das, D.; Gray, J. W.; Groves, J. T. *Science* **2010**, *327*, 1380−1385.
(14) DeMond, A. L.; Mossman, K. D.; Starr, T.; Dustin, M. L.; Groves, J. T. *Biophys. J.* **2008**, *94*, 3286−3292.
(15) Manz, B. N.; Jackson, B. L.; Petit, R. S.; Dustin, M. L.; Groves, J. T. *Proc. Natl. Acad. Sci. U.S.A.* **2011**, *108*, 9089−9094.
(16) Huppa, J. B.; Axmann, M.; Mörtelmaier, M. A.; Lillemeier, B. F.; Newell, E. W.; Brameshuber, M.; Klein, L. O.; Schütz, G. J.; Davis, M. M. *Nature* **2010**, *463*, 963−967.
(17) Dustin, M. L. *J. Struct. Biol.* **2009**, *168*, 152−160.
(18) Yu, Y.; Fay, N. C.; Smoligovets, A. A.; Wu, H.-J.; Groves, J. T. *PloS ONE* **2012**, *7*, e30704.
(19) Cemerski, S.; Das, J.; Giurisato, E.; Markiewicz, M. A.; Allen, P. M.; Chakraborty, A. K.; Shaw, A. S. *Immunity* **2008**, *29*, 414−422.
(20) Hartman, N. C.; Groves, J. T. *Curr. Opin. Cell Biol.* **2011**, *23*, 370−376.
(21) Li, P.; Banjade, S.; Cheng, H.-C.; Kim, S.; Chen, B.; Guo, L.; Llaguno, M.; Hollingsworth, J. V; King, D. S.; Banani, S. F.; Russo, P. S.; Jiang, Q.-X.; Nixon, B. T.; Rosen, M. K. *Nature* **2012**, *483*, 336−340.
(22) Bethani, I.; Skånland, S. S.; Dikic, I.; Acker-Palmer, A. *EMBO J.* **2010**, *29*, 2677−2688.
(23) Freywald, A.; Sharfe, N.; Roifman, C. M. *J. Biol. Chem.* **2002**, *277*, 3823−3828.
(24) Truitt, L.; Freywald, T.; DeCoteau, J.; Sharfe, N.; Freywald, A. *Cancer Res.* **2010**, *70*, 1141−1153.
(25) Janes, P. W.; Griesshaber, B.; Atapattu, L.; Nievergall, E.; Hii, L. L.; Mensinga, A.; Chheang, C.; Day, B. W.; Boyd, A. W.; Bastiaens, P. I.; Jørgensen, C.; Pawson, T.; Lackmann, M. *J. Cell Biol.* **2011**, *195*, 1033−1045.
(26) Janes, P. W.; Nievergall, E.; Lackmann, M. *Semin. Cell Dev. Biol.* **2012**, *23*, 43−50.
(27) Yarden, Y.; Sliwkowski, M. X. *Nat. Rev. Mol. Cell Biol.* **2001**, *2*, 127−137.
(28) Lemmon, M. A. *Exp. Cell Res.* **2009**, *315*, 638−648.
(29) Olayioye, M. A.; Neve, R. M.; Lane, H. A.; Hynes, N. E. *EMBO J.* **2000**, *19*, 3159−3167.
(30) Holmes, D. *Nat. Rev. Drug Discovery* **2011**, *10*, 798−800.
(31) Cochran, J. R. *Sci. Transl. Med.* **2010**, *2*, 17ps5.
(32) Saccà, B.; Meyer, R.; Erkelenz, M.; Kiko, K.; Arndt, A.; Schroeder, H.; Rabe, K. S.; Niemeyer, C. M. *Angew. Chem., Int. Ed.* **2010**, 9378−9383.
(33) Tepper, A. W. J. W. *J. Am. Chem. Soc.* **2010**, *132*, 6550−6557.
(34) Niemeyer, C. M.; Koehler, J.; Wuerdemann, C. *ChemBioChem* **2002**, *3*, 242−245.
(35) You, M.; Wang, R.-W.; Zhang, X.; Chen, Y.; Wang, K.; Peng, L.; Tan, W. *ACS Nano* **2011**, *5*, 10090−10095.
(36) Erkelenz, M.; Kuo, C.-H.; Niemeyer, C. M. *J. Am. Chem. Soc.* **2011**, *133*, 16111−16118.
(37) Yan, H.; Park, S. H.; Finkelstein, G.; Reif, J. H.; LaBean, T. H. *Science* **2003**, *301*, 1882−1884.
(38) Stephanopoulos, N.; Liu, M.; Tong, G. J.; Li, Z.; Liu, Y.; Yan, H.; Francis, M. B. *Nano Lett.* **2010**, *10*, 2714−2720.
(39) Yoshina-Ishii, C.; Miller, G. P.; Kraft, M. L.; Kool, E. T.; Boxer, S. G. *J. Am. Chem. Soc.* **2005**, *127*, 1356−1357.
(40) Selden, N. S.; Todhunter, M. E.; Jee, N. Y.; Liu, J. S.; Broaders, K. E.; Gartner, Z. J. *J. Am. Chem. Soc.* **2012**, *134*, 765−768.
(41) Galush, W. J.; Nye, J. A.; Groves, J. T. *Biophys. J.* **2008**, *95*, 2512−2519.
(42) Chen, Y.; Munteanu, A. C.; Huang, Y.-F.; Phillips, J.; Zhu, Z.; Mavros, M.; Tan, W. *Chem.—Eur. J.* **2009**, *15*, 5327−5336.
(43) Swift, J. L.; Godin, A. G.; Doré, K.; Freland, L.; Bouchard, N.; Nimmo, C.; Sergeev, M.; De Koninck, Y.; Wiseman, P. W.; Beaulieu, J.-M. *Proc. Natl. Acad. Sci. U.S.A.* **2011**, *108*, 7016−7021.
(44) Kempiak, S. J.; Yip, S.-C.; Backer, J. M.; Segall, J. E. *J. Cell Biol.* **2003**, *162*, 781−787.
(45) Plunkett, M.; Springer, T. *J. Immunol.* **1986**, *136*, 4181−4187.
(46) Hsiao, S. C.; Shum, B. J.; Onoe, H.; Douglas, E. S.; Gartner, Z. J.; Mathies, R. A.; Bertozzi, C. R.; Francis, M. B. *Langmuir* **2009**, *25*, 6985−6991.
(47) Twite, A. A.; Hsiao, S. C.; Onoe, H.; Mathies, R. A.; Francis, M. B. *Adv. Mater. (Weinheim, Ger.)* **2012**, *24*, 2380−2385.
(48) Onoe, H.; Hsiao, S. C.; Douglas, E. S.; Gartner, Z. J.; Bertozzi, C. R.; Francis, M. B.; Mathies, R. A. *Langmuir* **2012**, *28*, 8120−8126.
(49) Bacia, K.; Schwille, P. *Nat. Protoc.* **2007**, *2*, 2842−2856.
(50) Müller, B. K.; Zaychikov, E.; Bräuchle, C.; Lamb, D. C. *Biophys. J.* **2005**, *89*, 3508−3522.
(51) Chen, J.; Nag, S.; Vidi, P.-A.; Irudayaraj, J. *PloS ONE* **2011**, *6*, e17991.
(52) Slaughter, B. D.; Schwartz, J. W.; Li, R. *Proc. Natl. Acad. Sci. U.S.A.* **2007**, *104*, 20320−20325.
(53) Kettling, U.; Koltermann, A.; Schwille, P.; Eigen, M. *Proc. Natl. Acad. Sci. U.S.A.* **1998**, *95*, 1416−1420.
(54) Triffo, S. B.; Huang, H. H.; Smith, A. W.; Chou, E. T.; Groves, J. T. *J. Am. Chem. Soc.* **2012**, *134*, 10833−10842.
(55) Weidemann, T.; Wachsmuth, M. *Single Mol.* **2002**, *3*, 49−61.
(56) Chaudri, Z.; Bartlet-Jones, M.; Panayotou, G. *FEBS Lett.* **1999**, *450*, 23−26.
(57) Brennan, M.; Davison, P. F.; Paulus, H. *Science* **1985**, *229*, 81−83.
(58) Xu, Q.; Lin, W.-C.; Petit, R. S.; Groves, J. T. *Biophys. J.* **2011**, *101*, 2731−2739.
(59) Goodman, R. P.; Erben, C. M.; Malo, J.; Ho, W. M.; McKee, M. L.; Kapanidis, A. N.; Turberfield, A. J. *ChemBioChem* **2009**, *10*, 1551−1557.
(60) Nam, J.-M.; Nair, P. M.; Neve, R. M.; Gray, J. W.; Groves, J. T. *ChemBioChem* **2006**, *7*, 436−440.
(61) Jongsma, M. A.; Litjens, R. H. G. M. *Proteomics* **2006**, *6*, 2650−2655.